Characterization of mannitol in *Curvularia protuberata* hyphae by FTIR and Raman spectromicroscopy†

Merrill Isenor,[a] Susan G. W. Kaminskyj,[b] Russell J. Rodriguez,[cd] Regina S. Redman[ce] and Kathleen M. Gough*[a]

Received 16th July 2010, Accepted 21st September 2010
DOI: 10.1039/c0an00534g

FTIR and Raman spectromicroscopy were used to characterize the composition of *Curvularia protuberata* hyphae, and to compare a strain isolated from plants inhabiting geothermal soils with a non-geothermal isolate. Thermal IR source images of hyphae have been acquired with a 64 × 64 element focal plane array detector; single point IR spectra have been obtained with synchrotron source light. In some *C. protuberata* hyphae, we have discovered the spectral signature of crystalline mannitol, a fungal polyol with complex protective roles. With FTIR-FPA imaging, we have determined that the protein content in cells remains fairly constant throughout the length of a hypha, whereas the mannitol is found at discrete, irregular locations. This is the first direct observation of mannitol in intact fungal hyphae. Since the concentration of mannitol in cells varies with respect to position and is not present in all hyphae, this discovery may be related to habitat adaptation, fungal structure and growth stages.

Introduction

Fungal relationships with plants are ecologically diverse and many are essential. Endophyte and mycorrhizal fungi generate mutually beneficial interactions with living plants that have persisted for at least 450 million years and are thought to have been responsible for plant colonization of land.[1–3] These fungi are associated with at least 95% of plant species and play fundamental roles.[4,5] Mycorrhizae interact with plant roots, trading mineral nutrients scavenged from the soil for sugars from plant photosynthesis, and are important for plant survival and competition. Endophytes live asymptomatically within root and aerial plant tissues, creating interactions related to habitat adaptation. Unlike these mutualists, saprotrophs recycle dead materials, particularly plant cellulose and lignin that otherwise are resistant to degradation. We report here our spectroscopic evaluation of fungi associated with two ecological guilds: endophytes and saprotrophs. Conveniently, both of these types of fungi can be grown in pure culture on simple media.

Four fungal endophyte classes have been distinguished based on taxonomic group and metabolic effects related to plant colonization.[5] Class 2 endophytes are filamentous ascomycetes that colonize land plants growing in a diversity of natural conditions. Recently, several class 2 endophytes, including *Curvularia protuberata* strain Cp4666D, have been found to confer stress tolerance to plants growing in certain harsh habitats.[6,7] Habitat-adaptive fungal symbioses are essential for plant survival[5–7] and have been shown to colonize and confer comparable habitat tolerance to a broad range of plant species. Generally, habitat-adaptive endophytes increase plant drought tolerance and water use efficiency, hence, they could be important to agriculture. The physiological changes conferred to plants by fungal endophyte colonization are not fully understood.

The Cp4666D strain of *C. protuberata* was isolated from plants inhabiting geothermal soils that regularly reach 65 °C.[8] Its ability to confer thermal tolerance has been identified as an adaptation specific to geothermal habitats.[5–11] Notably, Cp4666D contains a double-stranded RNA virus (*Curvularia* thermal tolerance virus, CThTV) that is required for this effect. Neither a Cp4666D lacking the virus nor a *C. protuberata* strain from a culture collection could confer thermal tolerance.[9] Its presence is doubly necessary as neither the plant nor the fungus can tolerate these extreme temperatures on their own. The role of CThTV in this three-species symbiosis is not yet understood, nor is it known whether the virus affects fungal physiology when grown in culture, away from a host plant.

Fourier transform infrared (FTIR) spectromicroscopy is well suited to the examination of filamentous fungi,[12,13] providing spatially resolved information on cellular biochemical content. Fungi grow by extending hyphae that can be hundreds of microns long but only 2–10 μm in diameter. Hyphal growth occurs only at cell tips, by exocytosis, the localized secretion of wall materials, enzymes and nutrient-acquiring chemicals.[14,15] The result is a direct spatial relationship (distance from the hyphal tip) with age and cytoplasm function. Ultrastructure, composition and function can change substantially within a few micrometres. FTIR spectromicroscopic imaging makes it possible to probe these variations, relating composition to location within the cell. A greater understanding of cellular make-up is essential if we are to gain insight into the function of endophytes in the environment and the mechanism of habitat-adapted symbiosis.

In this paper, we characterize *C. protuberata* hyphae using spatially resolved FTIR spectromicroscopy, with the goal of comparing biochemical composition of geothermal and non-geothermal

[a]*Department of Chemistry, University of Manitoba, Winnipeg, Canada. E-mail: kmgough@cc.umanitoba.ca; Fax: +1 204-474-7608; Tel: +1 204-474-6262*
[b]*Department of Biology, University of Saskatchewan, Saskatoon, Canada*
[c]*US Geological Survey, Western Fisheries Research Center, Seattle, USA*
[d]*Department of Biology, University of Washington, Seattle, USA*
[e]*University of Washington, School of Forestry, Seattle, USA*
† This article is part of a themed issue on Optical Diagnosis. This issue includes work presented at SPEC 2010 Shedding Light on Disease: Optical Diagnosis for the New Millennium, which was held in Manchester, UK, June 26th to July 1st 2010.

isolates grown in culture. This composition is contrasted with three saprotroph species, nutrient scavengers that do not live symbiotically within plants, that we previously characterized with FTIR.[12,13] Our results show that saprotrophs and endophytes differ in their resource allocation. Many *C. protuberata* hyphae are found to contain mannitol, a six-carbon polyalcohol, known as a major carbohydrate component of fungal cytoplasm since the mid-1800s.[16] Despite being known for over a century, the role of mannitol in fungal metabolism, and even some aspects of its production and utilization, remain enigmatic.[16] Our work finds that mannitol is localized in hyphae; its distribution can easily be visualized in processed FTIR focal plane array (FPA) images.

Methods

Sample preparation

The habitat-adapted endophyte (Cp4666D) containing CThTV was isolated from geothermal plants; a non-geothermal isolate lacking the virus was obtained from the American Type Culture Collection (CpATCC). Blocks of potato dextrose agar (PDA) 100% growth medium, adjusted to pH 6.5 with NaOH and supplemented as needed with agar, were inoculated individually with spores. In order to study nutrient acquisition and allocation, some cultures were grown on diluted PDA (10%, 3% or 1%) amended with agarose for solidification. Agar blocks were placed on low-e MirrIR substrates (Kevley Technologies, www.kevley.com) or on gold-coated silicon wafers (University of Manitoba). Slides were incubated in moist chambers at 28 °C for 12–16 h, to allow growth of hyphae across clean substrate away from growth medium, then frozen at −80 °C and lyophilized to dryness. Hyphae of both isolates were grown on four separate occasions and plated onto dozens of separate substrates. For CpATCC and Cp4666D, 80 and 200 hyphae were examined, respectively.

A drop of mannitol was dissolved in distilled water, placed on a gold-coated silicon wafer and dried at room temperature to form thin crystals for IR reference spectra; loose crystals on a glass microscope slide served for Raman reference spectra.

Single point sFTIR spectra

Synchrotron FTIR (sFTIR) point spectra were collected in transflectance mode on the 031 mid-IR beamline at the Synchrotron Radiation Center (SRC) with a Nicolet Magna 550 interferometer and Continuum microscope with liquid nitrogen cooled MCT detector. OMNIC software was used for data collection and analysis. sFTIR spectra were also collected at the Canadian Light Source (CLS), on the 01B1-1 mid-IR beamline with a Bruker Optics IFS 66v/S interferometer and a Hyperion confocal microscope, with liquid nitrogen cooled MCT detector. Data acquisition was performed using the Opus software package. At both synchrotrons, the aperture was set to 10 × 10 μm for spectral acquisition at defined points along hyphae (typically hyphal tips and 30 μm, 50 μm, and 100 μm from tips). All spectra were collected at 4 cm^{-1} resolution between 4000 to 900 cm^{-1}. Between 256 and 2048 scans were co-added for each pixel and ratioed to a comparable background spectrum collected on a clean region of the slide. When necessary, an appropriately scaled water spectrum was subtracted from spectra.

FTIR-FPA imaging

Images were collected using a Varian 670 FTIR interferometer (Globar source) and Varian 620 imaging microscope with 64 × 64 element FPA MCT detector cooled with liquid nitrogen. Spectra were collected in transflectance with nominal 5.5 × 5.5 μm pixel resolution. Either 512 or 1024 scans were co-added and ratioed to a background collected on a clean area of the slide. Spectra were collected at 4 cm^{-1} resolution in the mid-IR region from 4000 to 900 cm^{-1}. The Varian Resolutions Pro software was used for data acquisition and analysis.

Raman spectra

Raman spectra were collected with a Renishaw inVia Raman microscope with a 50× objective. Point spectra were collected at hyphal tips as well as at 30 μm and 50 μm behind tips. A 785 nm diode laser, 1200 l mm^{-1} grating, was used for excitation; 256 scans, 4 s per scan, were co-added. Back-scattered light was collected on an electronically cooled CCD. The Renishaw WiRE software was used for data acquisition and analysis.

Results

Photographs of typical CpATCC hyphae grown from 100% and 10% PDA, and sFTIR spectra collected at 30 μm, 50 μm, and 100 μm behind tips, are shown in Fig. 1. In all figures, spectra are displayed on a common scale, offset for clarity. Spectra in Fig. 1b contain a slightly greater amount of both resonant and non-resonant Mie scatter. This well-known artefact can be corrected[17–20] but does not affect our overall analysis. The weakness of the fatty acid ester carbonyl absorption at 1740 cm^{-1} shows that lipid content is low. The absorption intensities in protein and sugar regions are similar at all positions. This trend of evenly distributed allocation was observed for most CpATCC and Cp4666D hyphae. Spectra from Cp4666D hyphae grown from 100% and 10% PDA were also very similar.[21]

Photographs and selected FTIR-FPA spectra are shown in Fig. 2a and b. FPA images were processed to show area under the amide I band (1666–1610 cm^{-1}; baseline 1711–1480 cm^{-1}) (Fig. 2c), and the sugar region (1085–1022 cm^{-1}; baseline 1138–982 cm^{-1}) (Fig. 2d). The spatial resolution decreases with increasing wavelength, hence the hyphal image is broadened slightly relative to the white light photograph. As expected, the raw transflectance signal increases where the hyphae overlap. Interestingly, the intensity from one hypha (points A and D) is lower than that from the other (points B and C). This has been observed in other hyphae, and may be due to different growth or nutritional status; however, the biochemical signatures are still similar.

The sFTIR and FTIR-FPA spectra of some hyphae contained unusual sharp peaks at ~1078 and 1022 cm^{-1}, often accompanied by weaker peaks at 1050 and 930 cm^{-1}. These were eventually attributed to crystalline mannitol following a literature search, and confirmed with IR and Raman reference spectra. Typical IR spectra from several positions along a Cp4666D hypha and a spectrum of mannitol are displayed in Fig. 3a. Raman spectra

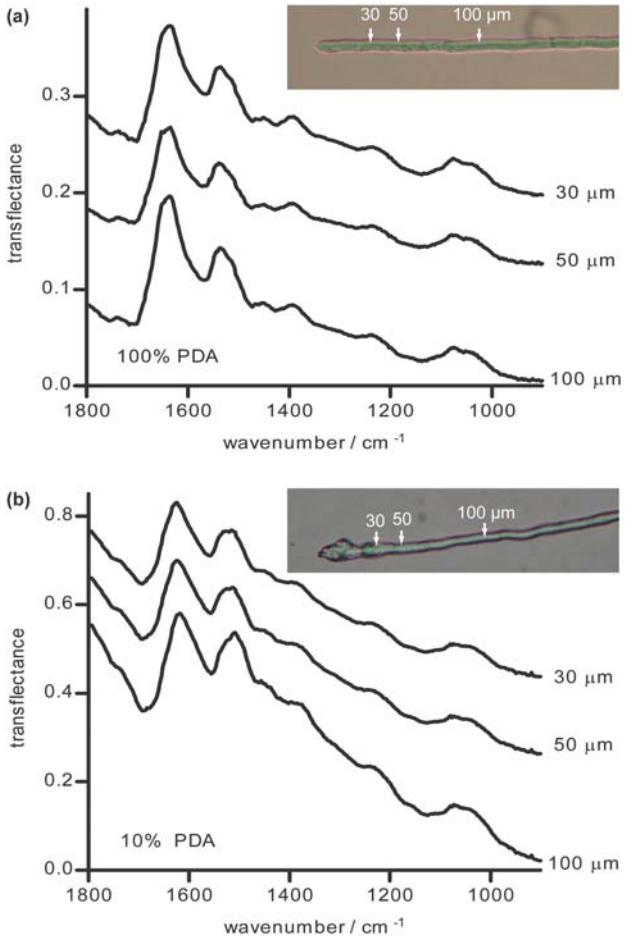

Fig. 1 Single pixel sFTIR spectra (SRC) collected from points 30, 50 and 100 µm behind the tip of CpATCC hyphae grown from (a) 100% and (b) 10% PDA.

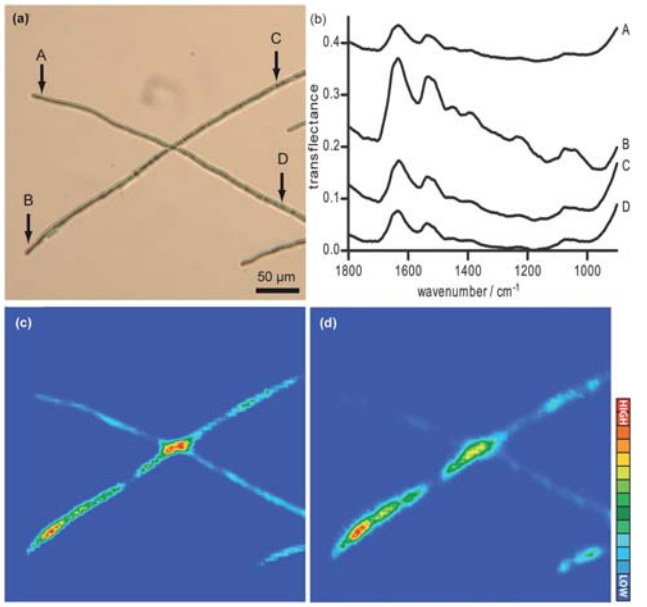

Fig. 2 (a) Photograph of two CpATCC hyphae grown from 100% PDA. (b) Selected FTIR spectra from hyphal tips and mature regions. FTIR-FPA images processed to show area under (c) the amide I band and (d) the carbohydrate region.

from two hyphae, one with and one without mannitol, and a Raman spectrum of pure mannitol are shown in Fig. 3b. Both hyphal spectra were collected 50 µm behind the tip. The peak at 1003 cm^{-1} (asterisk), present in all *C. protuberata* Raman spectra, is assigned to phenylalanine, a marker for protein.

Mannitol detection in the hypha was based on the IR bands at 1078, 1050, 1022, and 930 cm^{-1}. Fig. 4 shows two sFTIR spectra collected at the same position on a hypha with an aperture of 14 × 18 µm. For the second spectrum, the slide was rotated by 90°. The relative intensities of the bands at 1078 and 1022 cm^{-1} change with hyphal orientation relative to the polarized synchrotron source, signifying that the mannitol is present as oriented crystals. The status of mannitol in a living hypha may or may not be crystalline.

Comparison of FPA images of CpATCC and Cp4666D hyphae revealed that mannitol could be found in both isolates. FPA images of morphologically similar hyphae (Fig. 5a and b) were processed for the area under the amide I band. The protein allocation in both hyphae is fairly constant along the length (Fig. 5c and d) (c: 1666–1610 cm^{-1}; baseline 1711–1479 cm^{-1} and d: 1558–1613 cm^{-1}; baseline 1688–1480 cm^{-1}), consistent with data in Fig. 2. When processed to show mannitol (Fig. 5e and f) (e: 1088–1068 cm^{-1}; baseline 1119–974 cm^{-1} and f: 1027–1012 cm^{-1}; baseline 1117–978 cm^{-1}), the polyol is found at varying locations within hyphae, more abundantly in Cp4666D. Some 20% of the CpATCC hyphae were found to have at least one mannitol spot, compared to 40% of the Cp4666D hyphae. In contrast to the CpATCC, when detected, the Cp4666D usually had numerous mannitol locations, often close to the growing tip. Selected spectra were extracted (Fig. 5g and h) showing the presence or absence of mannitol bands.

Discussion

This study illustrates different modes of nutrient acquisition and metabolite allocation for different fungi. With sFTIR, we had shown that the biochemical content of saprotrophic *Aspergillus*, *Neurospora*, and *Rhizopus* hyphal tips is substantially less than in their more basal regions.[12,13] The important message is that low biochemical content is not correlated with low physiological activity, since it is well established that all growth is at the cell tip.[14,15]

Unexpectedly, the distribution was different for *C. protuberata* hyphae, where tips typically had a composition similar to regions >100 µm back and considered to be mature, thus the biochemical allocation along the length of hyphae was fairly even. *C. protuberata* appears to have a frugal metabolism since it is readily isolated and maintained on the nutritionally dilute 10% PDA,[9] unlike saprotrophic species that grow poorly. We found that fewer spores germinated from the lower (3% and 1%) PDA concentrations for both CpATCC and Cp4666D, but hyphal composition was unaffected.[21] The difference in the composition of saprotroph and endophyte hyphae could be a result of their different lifestyles. We note that all our endophytes were grown saprotrophically in our cultures, thus the behavior was not determined by environment.

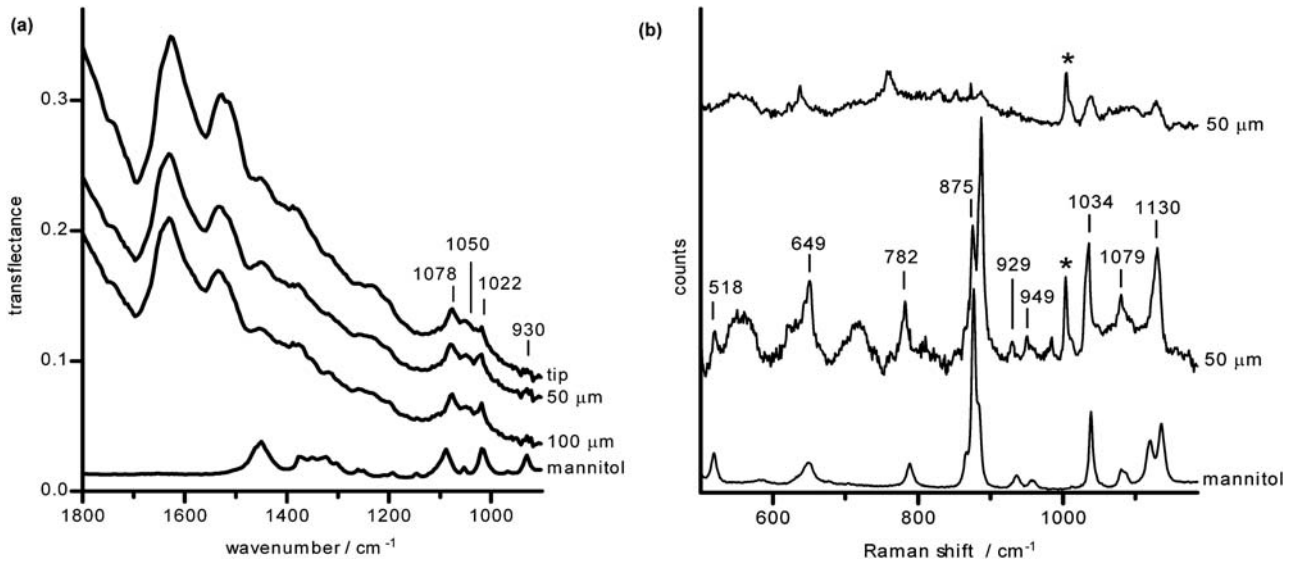

Fig. 3 Reference spectra of crystalline mannitol and (a) sFTIR spectra (CLS) collected from a Cp4666D hypha with irregular mannitol deposits, (b) Raman spectra collected 50 μm behind tips from two different Cp4666D hyphae, top without and middle with mannitol.

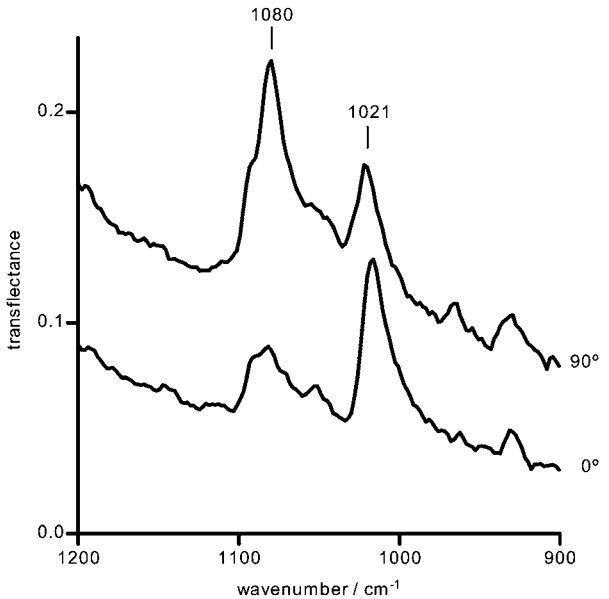

Fig. 4 sFTIR spectra (SRC) collected from the same position, 70 μm behind the hyphal tip, of a Cp4666D hypha. Upper and lower spectra correspond to slide oriented at 0° and 90° relative to polarized synchrotron beam.

In general, regions of increased protein content also contain more carbohydrate. The processed FPA image in Fig. 2 shows that cellular composition can vary between two neighbouring hyphae grown under the same conditions. One of the CpATCC hyphae actually had a slightly increased overall protein and sugar content in the apical region compared to areas farther back (Fig. 2, tip B). It is possible that the two hyphae were in different stages of development or metabolic activity when frozen.[22]

The two most prominent, sharp mannitol peaks in the IR spectra of *C. protuberata* hyphae have maxima ranging from 1018–1024 cm^{-1} and 1076–1081 cm^{-1}. Positions between 1019–1025 cm^{-1} and 1081–1088 cm^{-1} are reported; both positions and relative intensities depend on the polymorphic form, of which three have been identified.[23,24] The crystalline form of the reference mannitol in IR and Raman spectra, Fig. 3, is probably the β form, also known as modification I.[23] The crystals in the hypha resemble the α form (modification II), but both forms may be present; interference from the other biochemical components obscures some details. The β form is the more common and most stable for temperatures above 20 °C.[23] The α form can be obtained by rapid (10 °C min^{-1}) cooling of the β form after melting; in contrast, the delta form requires slow cooling.[23] While the mix of α and β may be the natural forms in the living hyphae, the α crystalline form could also be due to the manner of sample harvest (freezing for 30 minutes at −80 °C).

The literature IR and Raman mannitol spectra were not recorded with a polarized source.[23,24] We find that the relative intensities for sFTIR crystalline mannitol in hyphae change when the sample is rotated with respect to the polarized source (Fig. 4); this accounts for some of the variations in band intensities seen in our sFTIR spectra (polarized source). The Raman spectrum of mannitol has also been determined to be dependent on source polarization.[21]

We have detected mannitol in both CpATCC and Cp4666D hyphae; however, it is not present in spectra from all hyphae (*e.g.* Fig. 1 and 2).[21] Our data so far indicate that content is greater in the Cp4666D geothermal isolate. Mannitol is an extremely common polyol in nature and is widespread in septate fungi (fungi with cross-walls that divide the hypha into compartments).[16,25–27] However, mannitol has not been reported from aseptate fungi,[28] nor from unicellular *Saccharomyces cerevisiae*,[16] at least in the yeast phase of experimental strains. The abundance of mannitol in fungi varies from one species to another, but can range from 10% to 50% of the dry weight of various structures.[29–31]

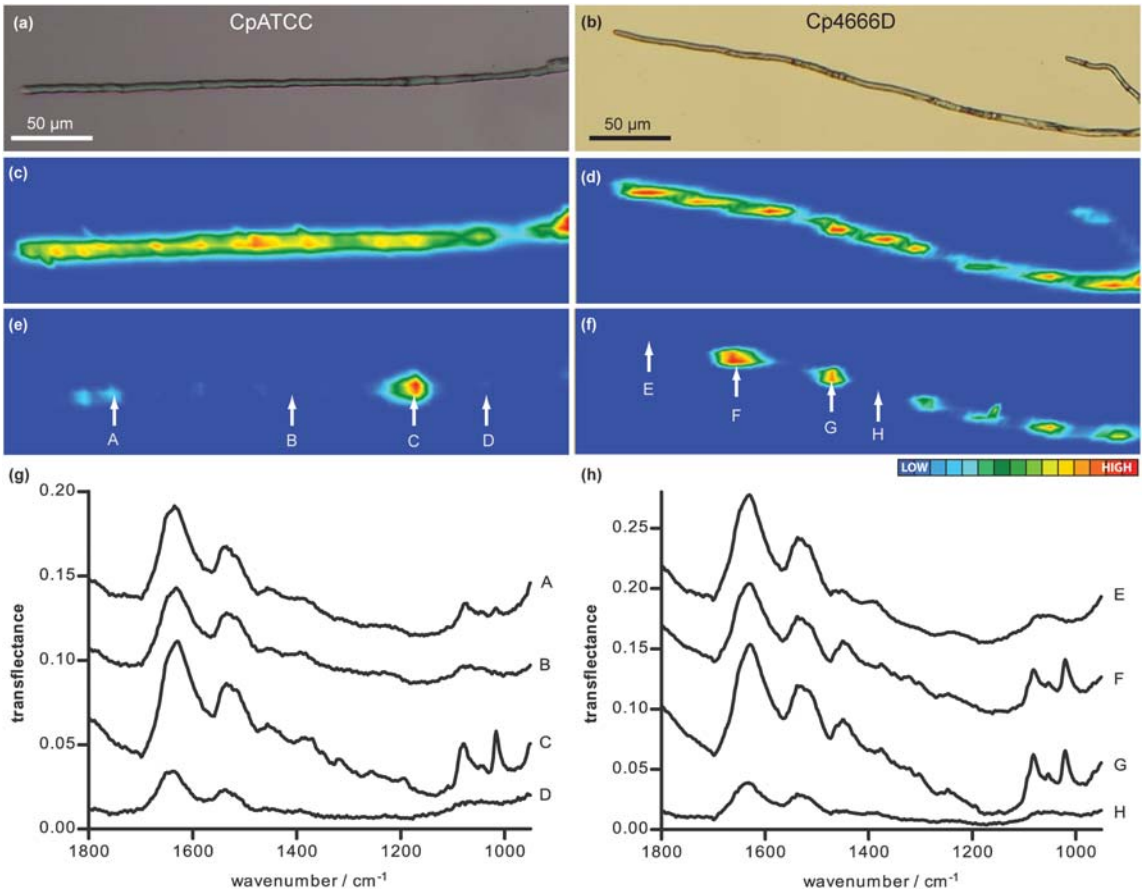

Fig. 5 Photographs of (a) CpATCC and (b) Cp4666D hyphae. FPA images were processed to show (c and d) protein distribution and (e and f) mannitol distribution. (g and h) FTIR-FPA spectra extracted from images at points A–D and E–H.

Based on its high abundance and wide distribution in septate fungi, mannitol is assumed to be metabolically important; however, numerous, diverse metabolic functions have been identified in saprotrophic and plant pathogenic fungi. It has been proposed as a nutrient store in *Aspergillus clavatus*,[32] *Stagonospora nodorum*,[33] *Uromyces fabae*,[34] and *Alternaria alternata*.[35] It is suggested to be important for stress tolerance in *Aspergillus niger*[30] and in *Cryptococcus neoformans*,[36] both of which can be facultative human pathogens. Mannitol has been found to protect fungi from reactive oxygen species[16,25] and is elevated during plant invasion.[33,34] Our observation of localized mannitol in hyphae could be one aspect of the geothermal protection. Further studies, including the analysis of live specimens, could offer a better understanding of when, where, and why mannitol is present in hyphae and whether its form is crystalline or dissolved in living cells.

Conclusions

We have presented the first spatially resolved FTIR characterization of hyphae from geothermal and non-geothermal isolates of the endophyte *C. protuberata*. These endophytes allocate resources evenly within growing hyphae, in contrast to saprotrophic species that we have examined, potentially due to their different lifestyles. Crystalline mannitol has been identified in some hyphae from both isolates, more abundantly in the geothermal type. The mannitol is found at discrete, irregular locations; it may play a role in thermal protection, not only in this fungus, but potentially in other fungal species as well. It may also be indicative of different growth phases of hyphae.

Acknowledgements

This research was supported by grants from NSERC to KMG and SGWK. The authors are grateful to L. Tzadu, Dr. S. Gajjeraman (U. Manitoba), X. Bao (U. Saskatchewan), Dr. R. Julian (SRC), Dr. Luca Quaroni and Dr. Tim May (CLS) for assistance with data collection. MI has been supported by the CIHR ITMHRT strategic training program, a Manitoba Graduate Scholarship and an NSERC CGS-M scholarship. This work is based in part upon research conducted at the Synchrotron Radiation Center, University of Wisconsin–Madison, which is supported by the National Science Foundation under award no. DMR-0537588. Additional support was provided by the US Geological Survey, NSF (0414463), and ARO (54120-LS). The use of trade, firm, or corporation names in this publication is for the information and convenience of the reader. Such use does not constitute an official endorsement or approval by the US Department of Interior or the US Geological Survey of any product or service to the exclusion of others that may be suitable.

References

1 K. A. Pirozynski and D. W. Malloch, *Biosystems*, 1975, **6**, 153–164.
2 D. W. Malloch, K. A. Pirozynski and P. H. Raven, *Proc. Natl. Acad. Sci. U. S. A.*, 1980, **77**, 2113–2118.
3 M. Krings, T. N. Taylor, H. Hass, H. Kerp, N. Dotzler and E. J. Hermsen, *New Phytol.*, 2007, **174**, 648–657.
4 S. E. Smith, and D. J. Read, *Mycorrhizal Symbiosis*, Academic Press, New York, 2nd edn, 1997.
5 R. J. Rodriguez, J. F. White Jr., A. E. Arnold and R. S. Redman, *New Phytol.*, 2009, **182**, 314–330.
6 R. J. Rodriguez, J. Henson, E. Van Volkenburgh, M. Hoy, L. Wright, F. Beckwith, Y.-O. Kim and R. S. Redman, *ISME J.*, 2008, **2**, 404–416.
7 R. Rodriguez and R. Redman, *J. Exp. Bot.*, 2008, **59**, 1109–1114.
8 R. S. Redman, K. B. Sheehan, R. G. Stout, R. J. Rodriguez and J. M. Henson, *Science*, 2002, **298**, 1581.
9 L. M. Márquez, R. S. Redman, R. J. Rodriguez and M. J. Roossinck, *Science*, 2007, **315**, 513–515.
10 R. J. Rodriguez, R. S. Redman and J. M. Henson, in *The Fungal Community: Its Organization and Role in the Ecosystem*, ed. J. Dighton, J. F. White, Jr and P. Oudemans, Taylor and Francis Group, Boca Raton, 2005, pp. 683–695.
11 R. J. Rodriguez, R. S. Redman and J. M. Henson, *Mitigation and Adaptation Strategies for Global Change*, 2004, **9**, 261–272.
12 A. Szeghalmi, S. Kaminskyj and K. M. Gough, *Anal. Bioanal. Chem.*, 2007, **387**, 1779–1789.
13 K. Jilkine, K. M. Gough, R. Julian and S. G. W. Kaminskyj, *J. Inorg. Biochem.*, 2008, **102**, 540–546.
14 *The Growing Fungus*, ed. N. A. R. Gow and G. M. Gadd, Chapman and Hall, London, 1995.
15 *Tip Growth in Plant and Fungal Cells*, ed. I. B. Heath, Academic Press, Toronto, 1990.
16 P. S. Solomon, O. D. C. Waters and R. P. Oliver, *Trends Microbiol.*, 2007, **15**, 257–262.
17 B. J. Davis, P. S. Carney and R. Bhargava, *Anal. Chem.*, 2010, **82**, 3474–3486.
18 B. J. Davis, P. S. Carney and R. Bhargava, *Anal. Chem.*, 2010, **82**, 3487–3499.
19 P. Bassan, H. J. Byrne, F. Bonnier, J. Lee, P. Dumas and P. Gardner, *Analyst*, 2009, **134**, 1586–1593.
20 P. Bassan, A. Kohler, H. Martens, J. Lee, H. J. Byrne, P. Dumas, E. Gazi, M. Brown, N. Clarke and P. Gardner, *Analyst*, 2010, **135**, 268–277.
21 M. Isenor, MSc. thesis, University of Manitoba, 2010.
22 M. Hubbard and S. Kaminskyj, *Mycol. Prog.*, 2007, **6**, 179–189.
23 A. Burger, J.-O. Henck, S. Hetz, J. M. Rollinger, A. A. Weissnicht and H. Stöttner, *J. Pharm. Sci.*, 2000, **89**, 457–468.
24 P. Ye and T. Byron, *Am. Lab. (Shelton, CT, U. S.)*, 2008, **40**, 24–27.
25 T. Dulermo, C. Rascle, G. Billon-Grand, E. Gout, R. Bligny and P. Cotton, *Biochem. J.*, 2010, **427**, 323–332.
26 S. H. Song and C. Vieille, *Appl. Microbiol. Biotechnol.*, 2009, **84**, 55–62.
27 C. F. B. Witteveen and J. Visser, *FEMS Microbiol. Lett.*, 1995, **134**, 57–62.
28 H. Abro, H. A. M. Crowther, C. J. Lawson and M. W. Dick, *Biochem. Syst. Ecol.*, 1989, **17**, 439–441.
29 D. Rast, *Planta*, 1965, **64**, 81–93.
30 G. J. G. Ruijter, M. Bax, H. Patel, S. J. Flitter, P. J. I. van de Vondervoort, R. P. de Vries, P. A. van Kuyk and J. Visser, *Eukaryotic Cell*, 2003, **2**, 690–698.
31 H. Yamada, K. Okamoto, K. Kodama, F. Noguchi and S. Tanaka, *J. Biochem.*, 1961, **49**, 404–410.
32 D. L. Corina and K. A. Munday, *J. Gen. Microbiol.*, 1971, **69**, 221–227.
33 P. S. Solomon, K. C. Tan and R. P. Oliver, *Mol. Plant–Microbe Interact.*, 2005, **18**, 110–115.
34 R. T. Voegele, M. Hahn, G. Lohaus, T. Link, I. Heiser and K. Mendgen, *Plant Physiol.*, 2005, **137**, 190–198.
35 H. Velez, N. J. Glassbrook and M. E. Daub, *Fungal Genet. Biol.*, 2007, **44**, 258–268.
36 V. Chaturvedi, B. Wong and S. L. Newman, *J. Immunol.*, 1996, **156**, 3836–3840.